



Research Article

ISSN : 0975-7384
CODEN(USA) : JCPRC5

Formaldehyde (CH₂O) removal assisted by vapor and oxygen gas through pulse discharge method

Lianshui Zhang, Xiaojun Wang^{*}, Weidong Lai and Xiaomin Feng

College of Physics Science and Technology, Hebei University, Baoding, Hebei Province, P. R. China

ABSTRACT

Though formaldehyde (CH₂O) is the highly consumed organic chemical reactant in the world, its toxicity to human being has drawn much attention. CH₂O removal is important for in-door air quality improvement. In this article, the CH₂O removal dynamic process is simulated through pulse discharge method by establishing a zero dimensional model. Simulation indicates that the H₂O vapor additive have achieved CH₂O removal by generating OH and H radicals after electron collision, though H₂O concentration ratio should be high for achieving effective removal. The mixing ratio increments of H₂O can accelerate the generation of benign species of CO₂ rather than CO through the reactions of OH with HCO radical and CO. The O₂ additive is more efficient for achieving higher removal efficiency at lower mixing ratio than that H₂O additive. When both H₂O and O₂ are co-mixed with CH₂O, there appears reproduction of CH₂O induced by the reaction between H₂O molecule and HCO radical, which arises out the attenuation effect on the CH₂O removal process.

Keywords: Formaldehyde, gas additive, removal, pulse discharge, simulation

INTRODUCTION

Environmental pollution on air, water or soil are dramatically deteriorating the living conditions of human beings [1-2], and there have many researches on the pollutant ingredients treatment methods such as catalyzing at high temperature, electrochemically oxidizing and so on [3-5]. As an important component of the volatile organic compounds (VOCs), formaldehyde with the chemical structure of CH₂O or HCHO has been consumed at very large quantities as essential reactants for producing urea formaldehyde resin, melamine resin, phenol formaldehyde resin [6]. Except its widespread utilization in factories, the CH₂O has also been vastly applied as key ingredients in the household furniture, the building materials, the automobiles, the electrical systems, or even the textiles and clothes [7]. The CH₂O gas should assume important responsibility on the deteriorated indoor air quality [8]. Reports verify the toxicity of CH₂O that the upper respiratory tract or eyes of human being can be irritated by trace amount of CH₂O, or injured when more CH₂O inhaled. By ingesting as little as 30 ml, the solution containing 37% CH₂O can induce death of an adult [9]. Recently, *Salthammer* had reported a worse fact that even the CH₂O in outdoor air has sometimes reached to the indoor levels, particularly in polluted urban areas [10].

In order to remove the CH₂O gas, there have various kinds of treatment methods. Bio-trickling filters have been developed and practiced [11-12]. To adsorb the gas molecules, the mesoporous carbon material was prepared and activated by H₂SO₄ or NH₃ [13]. Photo-catalysis process is now recognized as an efficient method to remove gaseous VOCs [14-15], though with the drawback of light attenuation through scatter or absorption. Even indoor plants had been investigated for their CH₂O removal functions [16]. The discharge plasma technique is another candidate. *Saulich et al.* had developed a cycled adsorption and discharge process, through which the CH₂O molecules were firstly adsorbed by halloysite granules and secondly decomposed into CO_x by discharge [17]. In dielectric barrier discharge (DBD), the CH₂O molecule is more efficiently removed in nitrogen additive than in air at 20°C due to the efficient energy transfer from nitrogen metastable states [18]. The electrical discharge technique

possesses the advantages of high efficiency and low cost. Since additive gas can usually improve the removal process of pollutant gases under optimal mixing and discharging conditions [19-20], the CH₂O gas removal kinetics is simulated through pulse streamer discharge technique in this article, and the vapor and oxygen additive effect on CH₂O removal efficiency is focused on.

EXPERIMENTAL SECTION

The additive gases such as vapor (H₂O) or oxygen (O₂) are mixed with formaldehyde (CH₂O) at the premix gas tube, and then streamed into the discharge zone, in which high energy electrons are driven by pulse voltage and injected from the electrodes. The discharge energy is hypothesized as 147 Td. The CH₂O concentration is set as 1000 ppm to imitate the in-door air condition. Based on these hypotheses, the electrons collision on CH₂O is ignored due to the small concentrations. Contrarily, the H₂O or O₂ concentration is relatively high, and their electron collision process should be included.

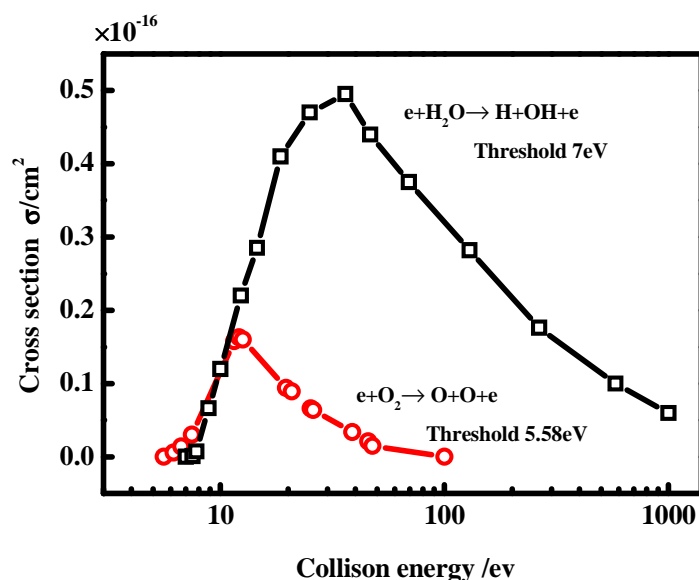


Fig. 1 Electron collision dissociative cross sections of H₂O and O₂. The dissociative energy threshold is 7 eV for H₂O and 5.58 eV for O₂

The electron collision dissociative cross sections of H₂O and O₂ are present in Fig. 1. The H₂O dissociative cross sections are obviously higher than that of O₂. But the O₂ molecule is easier to be decomposed by electron collision, due to its lower dissociative energy threshold.

By solving *Boltzmann* Equation of the collision cross sections [21], the dissociative rate coefficients of H₂O or O₂ molecule are calculated in this article as



After collision by high energy electrons, there have H, OH and O radicals generated, which can participate into the CH₂O removal process. The main reactions and the corresponding rate coefficients related to CH₂O removal are analyzed and outlined in Tab. 1 [22].

According to the outlined reaction paths and corresponding rate coefficients, the time-resolved concentration evolutions of all the species are modeled in this article as

$$\frac{dn_i}{dt} = -\sum_{i,j} k_{ij} n_i n_j + \sum_{p,q} k_{pq} n_p n_q \quad (3)$$

In which, the concentration variance of i^{th} specie is derived from its concentration losing process caused by the reaction between i^{th} and j^{th} species and the generating process caused by the reaction between p^{th} and q^{th} species. Every reaction is ruled by the rate coefficients of k_{ij} or k_{pq} .

Tab. 1 Main reactions and rate coefficients simulated in this article

R.	Reactions	$k / \text{cm}^3 \text{s}^{-1}$	R.	Reactions	$k / \text{cm}^3 \text{s}^{-1}$
1	$\text{CH}_2\text{O} + \text{O} \rightarrow \text{HCO} + \text{OH}$	6.73×10^{-11}	17	$\text{CO} + \text{O}_2 \rightarrow \text{CO}_2 + \text{O}$	1.43×10^{-13}
2	$\text{CH}_2\text{O} + \text{O} \rightarrow \text{CO} + \text{OH} + \text{H}$	1.00×10^{-10}	18	$\text{CO} + \text{OH} \rightarrow \text{CO}_2 + \text{H}$	3.90×10^{-12}
3	$\text{CH}_2\text{O} + \text{H} \rightarrow \text{H}_2 + \text{HCO}$	7.71×10^{-10}	19	$\text{CO} + \text{H} \rightarrow \text{HCO}$	5.70×10^{-34}
4	$\text{CH}_2\text{O} + \text{OH} \rightarrow \text{HCO} + \text{H}_2\text{O}$	8.13×10^{-12}	20	$\text{H}_2\text{O} + \text{H} \rightarrow \text{H}_2 + \text{OH}$	8.90×10^{-11}
5	$\text{HCO} + \text{O} \rightarrow \text{CO} + \text{OH}$	5.00×10^{-11}	21	$\text{OH} + \text{H} \rightarrow \text{H}_2\text{O}$	1.55×10^{-32}
6	$\text{HCO} + \text{O} \rightarrow \text{CO}_2 + \text{H}$	5.00×10^{-11}	22	$\text{OH} + \text{H} \rightarrow \text{H}_2 + \text{O}$	1.25×10^{-10}
7	$\text{HCO} + \text{H} \rightarrow \text{CO} + \text{H}_2$	1.50×10^{-10}	23	$\text{H}_2 + \text{OH} \rightarrow \text{H}_2\text{O} + \text{H}$	6.70×10^{-15}
8	$\text{HCO} + \text{H} \rightarrow \text{CH}_2\text{O}$	2.38×10^{-33}	24	$\text{H}_2 + \text{O} \rightarrow \text{OH} + \text{H}$	3.40×10^{-10}
9	$\text{HCO} + \text{H}_2\text{O} \rightarrow \text{CH}_2\text{O} + \text{OH}$	5.29×10^{-10}	25	$\text{H}_2 + \text{O}_2 \rightarrow \text{H}_2\text{O} + \text{O}$	1.45×10^{-13}
10	$\text{HCO} + \text{OH} \rightarrow \text{CO} + \text{H}_2\text{O}$	1.69×10^{-10}	26	$\text{H}_2 + \text{O}_2 \rightarrow \text{OH} + \text{OH}$	1.43×10^{-11}
11	$\text{HCO} + \text{HCO} \rightarrow \text{CO} + \text{CO} + \text{H}_2$	3.64×10^{-11}	27	$\text{O}_2 + \text{H} \rightarrow \text{OH} + \text{O}$	2.49×10^{-11}
12	$\text{HCO} + \text{HCO} \rightarrow \text{CH}_2\text{O} + \text{CO}$	5.00×10^{-11}	28	$\text{OH} + \text{O} \rightarrow \text{O}_2 + \text{H}$	1.51×10^{-11}
13	$\text{HCO} + \text{H}_2 \rightarrow \text{CH}_2\text{O} + \text{H}$	4.51×10^{-10}	29	$\text{O} + \text{O} \rightarrow \text{O}_2$	9.95×10^{-35}
14	$\text{CO}_2 + \text{O} \rightarrow \text{CO} + \text{O}_2$	5.22×10^{-13}	30	$\text{H} + \text{O} \rightarrow \text{OH}$	2.60×10^{-33}
15	$\text{CO}_2 + \text{H} \rightarrow \text{CO} + \text{OH}$	1.48×10^{-11}	31	$\text{H}_2\text{O} + \text{O} \rightarrow \text{OH} + \text{OH}$	4.83×10^{-11}
16	$\text{CO} + \text{O} \rightarrow \text{CO}_2$	1.25×10^{-33}			

It should be noticed that there have no components related to spatial variance, and time evolution is included. Such a model is only related to time, and is zero-dimensional. By solving the time varying differential equation system, the CH_2O removal kinetic process can be monitored. The *Runge-Kutta* algorithm is applied for such purpose [23].

RESULTS AND DISCUSSION

Based on the reaction model, H_2O or O_2 additives are the key factors for CH_2O removal through pulse streamer discharge. The favorite productions are expected benign or easy-captured for further processing. In this article, H_2O or $\text{H}_2\text{O}/\text{O}_2$ additive effect is respectively discussed.

The removal efficiency is defined as

$$\eta_{\text{CH}_2\text{O}} = \frac{n_0 - n_r}{n_0} \times 100\% \quad (4)$$

n_0 is the initial concentration of CH_2O , and n_r is the residual concentration after the simulation period. The initial CH_2O concentration is set as $2.457 \times 10^{16} \text{ cm}^{-3}$. The discharge duration is $0.5 \mu\text{s}$, and the total simulation period is $4 \mu\text{s}$.

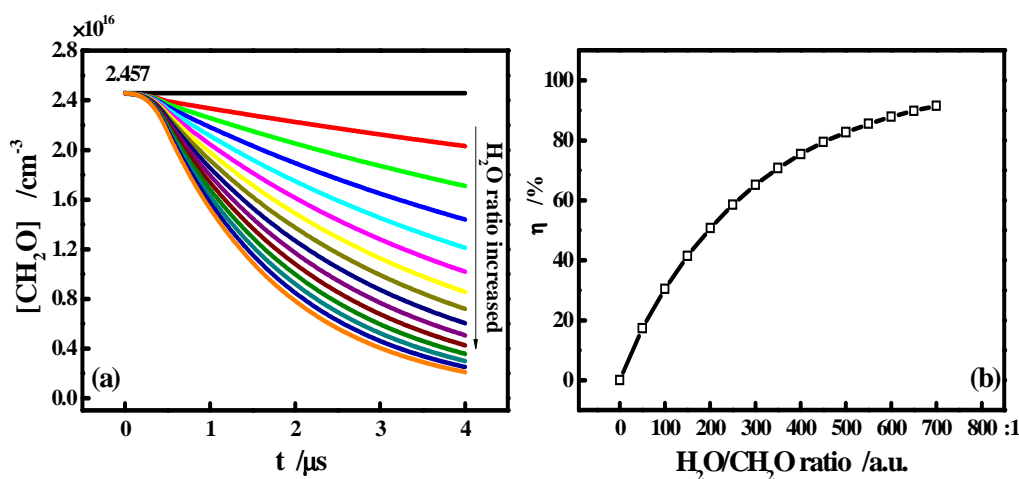


Fig. 2 At different $\text{H}_2\text{O}/\text{CH}_2\text{O}$ ratio, (a) time-resolved concentration evolution of CH_2O , and (b) the corresponding CH_2O removal efficiency

3.1 Effect of H_2O vapor additive on CH_2O removal kinetics

When only H_2O vapor are mixed, the time-resolved concentration evolutions of CH_2O are simulated in Fig. 2a, which decreases at a monotonic trend and CH_2O removal has been achieved. When it comes to the H_2O additive effect, the higher the H_2O vapor concentration ratio is, the more the CH_2O molecules are removed. It should be noticed that the major removal process is occurred after $0.5 \mu\text{s}$, which indicates that the radicals produced during

discharge have effectively participated into the further reactions after discharge. This is due to the uniform distribution hypothesis that the spatial drift of all gaseous species are ignored, and they can react with each other at unit space during and after discharge.

The removal efficiency η is calculated in Fig. 2b. With concentration ratio between H₂O and CH₂O heightened, the removal process is remarkably accelerated. Removal efficiency has achieved to 91.47% when the H₂O/CH₂O ratio is 750:1. Such removal is mainly decided by the H and OH radicals decomposed from H₂O as follows.



In order to clarify the main removal paths during and after discharge, the time-resolved concentration evolutions of OH and H radicals are present in Fig. 3.

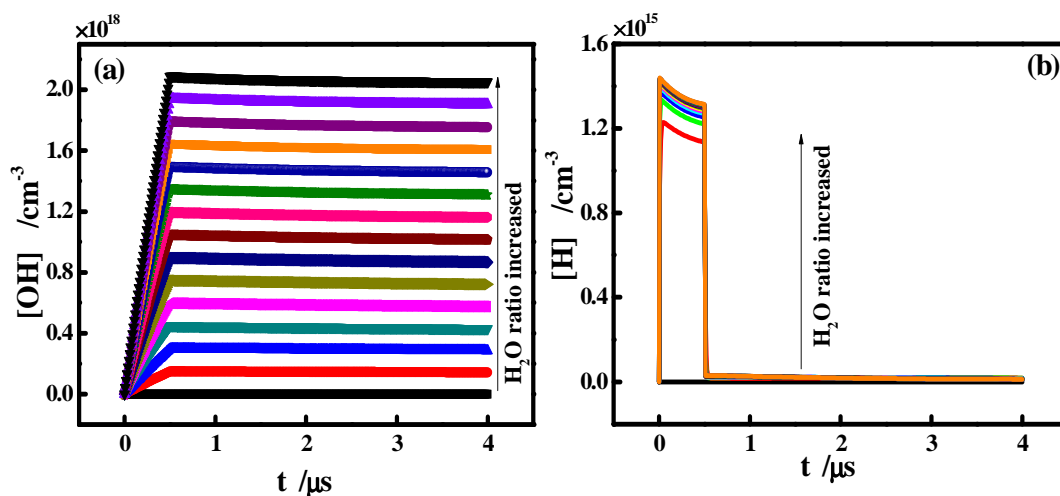


Fig. 3 At different H₂O/CH₂O ratio, (a) time-resolved concentration evolution of OH and (b) H radicals

There has more OH radicals been generated and preserved after discharge in Fig. 3a. For the H radical, it has been consumed out during discharge. Such evolutions indicate that the H and OH radicals have decided the CH₂O removal kinetics during discharge, and the OH is played the essential role for the CH₂O removal after discharge.

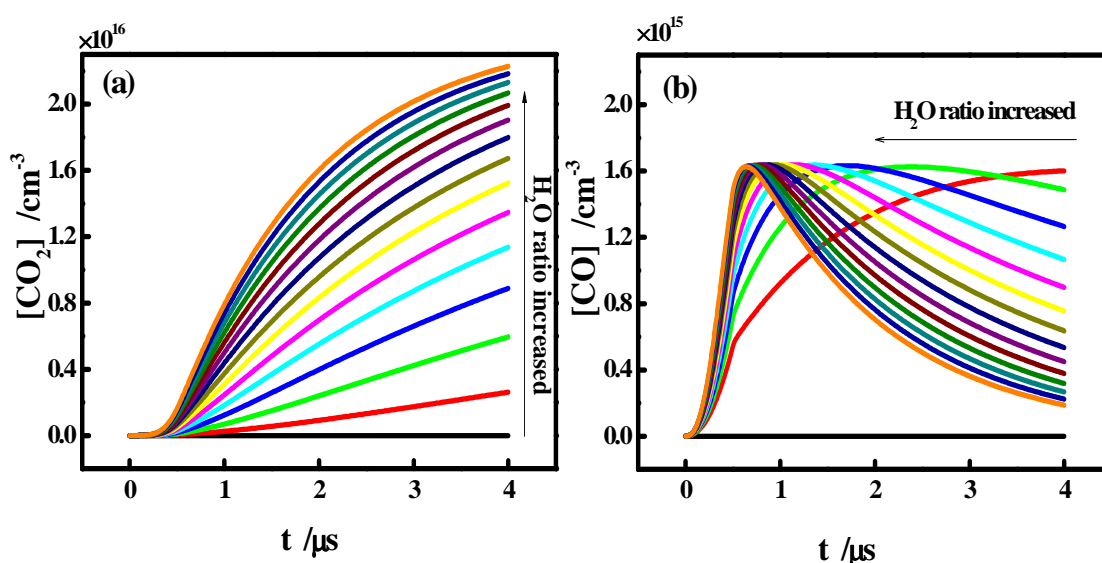


Fig. 4 At different H₂O/CH₂O ratio, (a) time-resolved concentration evolution of CO₂, and (b) time-resolved concentration evolution of CO

Since the CH₂O is an organic VOC compound with its chemical structure including C elements, it is important to

monitor the transformation of C in the final productions. Simulation presents that most of the C elements in CH₂O molecules have transformed into CO₂ rather than CO, as present in Fig. 4.

During the simulation period of 4μs, the CO₂ concentration is varied with monotone increasing trends. And its concentration is heightened when more H₂O added. Contrarily, the CO concentration at 4μs is decreased when H₂O concentration heightened. CO₂ is the major final production.

When it comes to the generation kinetics, the CO concentration evolution presents a first increasing then decreasing trend. During discharge, CO has been generated and accumulated. Even more CO molecules have been produced than CO₂ at discharge duration time of 0.5μs. The C elements in CH₂O molecules are first transformed into CO during discharge. For CO₂ production, except the CO oxidization by O₂ or O, there has another more important routine. The generated HCO radicals ruled by Equation 5 and 6 can react with OH to generate CO during and after discharge. And the CO molecule is further transformed into CO₂ through the reaction with OH. Such processes are the key factors for CO₂ generation after discharge, and shown as follows.



3.2 Effect of O₂ and H₂O co-additive on CH₂O removal kinetics

The oxygen and H₂O vapor are usually mixed together in ordinary gaseous environment. Then one question is put forward how the two components influence each other when both gases are added into CH₂O.

In Fig. 5, without H₂O mixing, the O₂ can achieve effective CH₂O removal at lower ratio than that of H₂O additive. At H₂O/O₂/CH₂O ratio of 0:16:1, the removal efficiency becomes 98.7%. The O radicals decomposed from O₂ are more efficient for CH₂O removal.

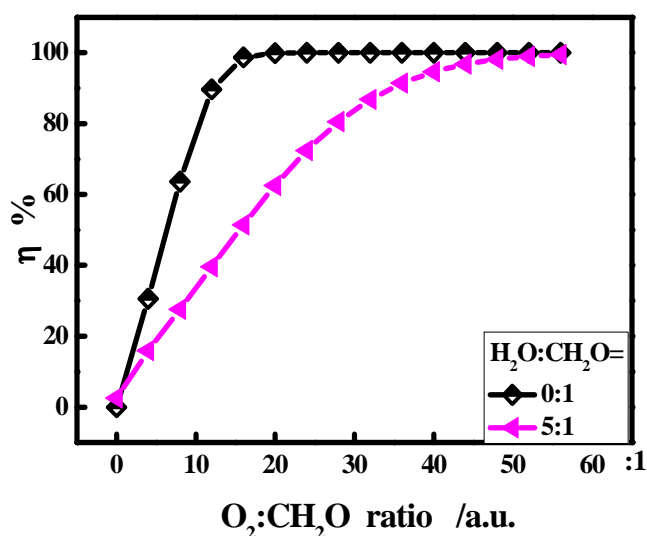


Fig. 5 At different O₂/CH₂O mixing ratio, the CH₂O removal efficiency achieved without or with small portion of H₂O vapor additive

But the CH₂O removal efficiency is obviously affected by H₂O vapor co-additive, though the concentration ratio of H₂O/CH₂O is very small as 5:1. The removal effect of O₂ on CH₂O has been greatly attenuated in Fig. 5. There should have more O₂ molecules to participate into the removal reactions in order to achieve the same removal efficiency. Such attenuation is ascribed to the reversal reaction caused by H₂O, for reproducing the CH₂O from CHO radicals ruled by



According to Equation 9, more H₂O vapor additive would induce the aggravating attenuation on CH₂O removal kinetics, as shown in Fig. 6.

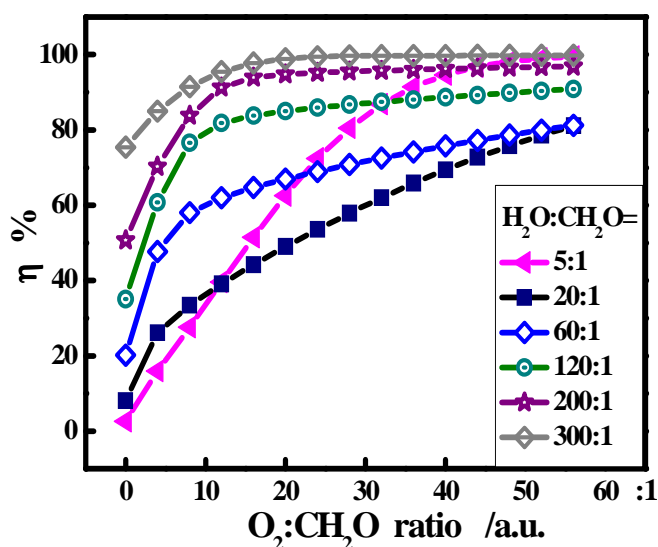


Fig. 6 At different O₂/CH₂O mixing condition, the CH₂O removal efficiency achieved under different ratio of H₂O vapor co-additive

When more H₂O added, for example at the H₂O/CH₂O ratio of 20:1, the maximal removal efficiency has been greatly attenuated and decreased to 81.17%. With vapor concentration further heightened, the removal efficiency at low O₂ concentration ratio has been improved. The higher the H₂O concentration ratio is, the higher the removal efficiency at lower O₂ ratio becomes. H and OH radicals decomposed from H₂O have played more and more important roles for CH₂O removal. Under H₂O/CH₂O ratio of 300:1, the removal efficiency has become 98.9% at O₂/CH₂O ratio of 20:1, though it is also slightly lower than that without H₂O additive of 99.9%.

CONCLUSION

CH₂O removal dynamic process is simulated in this article through pulse streamer discharge method. After establishing a zero dimensional reaction model, the CH₂O removal process is monitored. Results indicate that the H and OH decomposed from H₂O have played important roles for CH₂O removal, though the H₂O concentration is relatively high for achieving effective removal. Higher additive ratio of H₂O can adjust the reactions for generating more benign species of CO₂. OH radicals have decided the most part of CO₂ generation through the reactions with HCO radical and CO. The O₂ additive is more efficient for achieving higher removal effect at lower mixing ratio than that H₂O additive. When H₂O is co-mixed with O₂, attenuation on CH₂O removal kinetic are induced by reproducing CH₂O through the reaction between HCO radical and H₂O molecule.

The formaldehyde (CH₂O) removal treatment through pulse discharge method is important for air quality improvement, and there should have further investigation on its kinetics in order to obtain optimal discharging conditions for practical utilization.

Acknowledgments

This work is financially supported by National Nature Science Foundation of China No. 10875036, and the Nature Science Foundation of Hebei Province No. A2007000131, A2010000177.

REFERENCES

- [1] S Gnanasekaran; K Subramani; AT Ansari. *J. Chem. Pharm. Res.*, **2010**, 2(5), 153-160.
- [2] A Mao; EB Hassan; MG Kim. *BioResour.*, **2013**, 8(2), 2453-2469.
- [3] PMN Prasad; ES Sundar; RCK Reddy; VH Reddy; YVR Reddy. *J. Chem. Pharm. Res.*, **2012**, 4(6), 2999-3002.
- [4] S Chauhan. *J. Chem. Pharm. Res.*, **2010**, 2(4), 489-495.
- [5] OIDEI Mouden; M Errami; R Salghi; A Zarrouk; M Assouag; H Zarrouk; SS Al-Deyab; B Hammouti. *J. Chem. Pharm. Res.*, **2012**, 4(7), 3437-3445.
- [6] G Reuss; W Disteldorf; A Gamer; A Hilt. Formaldehyde. *Ullmann's Encyclopedia of Industrial Chemistry*, **2000**, DOI: 10.1002/14356007.a11_619.
- [7] S Kim; YK Choi; KW Park; JT Kim. *Bioresour. Technol.*, **2010**, 101(16), 6562-6568.
- [8] DA Sarigiannis; SP Karakitsios; A Gotti. *Fresenius Environ. Bull.*, **2012**, 21(11), 3160-3167.

- [9] ATSDR (Agency for Toxic Substances & Disease Registry). Medical Management Guidelines for Formaldehyde, **2013**, URL: <http://www.atsdr.cdc.gov/mmg/mmg.asp?id=216&tid=39>.
- [10] T Salthammer. *Angew. Chem. Int. Ed.*, **2013**, 52(12), 3320-3327.
- [11] M Fulazzaky; A Talaiekhosravi; T Hadibarata. *RSC Adv.*, **2013**, 3(15), 5100-5107.
- [12] JM Garrido; R Mendez; JM Lema. *Water Res.*, **2001**, 35(3), 691-698.
- [13] HB An; MJ Yu; JM Kim; MS Jin; JK Jeon; SH Park; SS Kim; YK Park. *Nanoscale Res. Lett.*, **2012**, 7, 7-12.
- [14] PA Bourgeoi; E Puzenat; L Peruchon; F Simonet; D Chevalier; E Deflin; C Brochier; C Guillard. *Appl. Catal. B: Environ.*, **2012**, 128, 171-178.
- [15] P Chin; LP Yang; DF Ollis. *J. Cata.*, **2006**, 237(1), 29-37.
- [16] A Aydogan; LD Montoya. *Atmos. Environ.*, **2011**, 45(16), 2675-2682.
- [17] K Saulich; S Müller. *J. Phys. D: Appl. Phys.*, **2013**, 46(4), 045201.
- [18] N Blin-Simiand; S Pasquiers; F Jorand; C Postel; JR Vacher. *J. Phys. D: Appl. Phys.*, **2009**, 42(12), 122003.
- [19] DH Lee; KT Kim; HS Kang; YH Song; JE Park. *Environ. Sci. Technol.*, **2013**, 47(19), 10964-10970.
- [20] FJ Beckers; WF Hoeben; AJ Pemen; EJ van Heesch. *J. Phys. D: Appl. Phys.*, **2013**, 46, 295201.
- [21] K Behringer; U Fantz. *J. Phys. D: Appl. Phys.*, **1994**, 27, 2128-2135.
- [22] NIST. NIST Chemical Kinetics Database: A compilation of kinetics data on gas-phase reactions, **2013**, URL: <http://kinetics.nist.gov/kinetics/index.jsp>.
- [23] J Butcher. Numerical methods for ordinary differential equations, New York: John Wiley & Sons, **2003**; 123-185.